JCBFM

Caloric restriction improves diabetes-induced cognitive deficits by attenuating neurogranin-associated calcium signaling in high-fat diet-fed mice

Hwajin Kim[1]*, Heeyoung Kang[2]*, Rok Won Heo[1],
Byeong Tak Jeon[3], Chin-ok Yi[1], Hyun Joo Shin[1],
Jeonghyun Kim[4], Seon-Yong Jeong[4], Woori Kwak[5],
Won-Ho Kim[6], Sang Soo Kang[1] and Gu Seob Roh[1]

Abstract

Diabetes-induced cognitive decline has been recognized in human patients of type 2 diabetes mellitus and mouse model of obesity, but the underlying mechanisms or therapeutic targets are not clearly identified. We investigated the effect of caloric restriction on diabetes-induced memory deficits and searched a molecular mechanism of caloric restriction-mediated neuroprotection. C57BL/6 mice were fed a high-fat diet for 40 weeks and RNA-seq analysis was performed in the hippocampus of high-fat diet-fed mice. To investigate caloric restriction effect on differential expression of genes, mice were fed high-fat diet for 20 weeks and continued on high-fat diet or subjected to caloric restriction (2 g/day) for 12 weeks. High-fat diet-fed mice exhibited insulin resistance, glial activation, blood–brain barrier leakage, and memory deficits, in that we identified *neurogranin*, a down-regulated gene in high-fat diet-fed mice using RNA-seq analysis; neurogranin regulates Ca^{2+}/calmodulin-dependent synaptic function. Caloric restriction increased insulin sensitivity, reduced high-fat diet-induced blood–brain barrier leakage and glial activation, and improved memory deficit. Furthermore, caloric restriction reversed high-fat diet-induced expression of neurogranin and the activation of Ca^{2+}/calmodulin-dependent protein kinase II and calpain as well as the downstream effectors. Our results suggest that neurogranin is an important factor of high-fat diet-induced memory deficits on which caloric restriction has a therapeutic effect by regulating neurogranin-associated calcium signaling.

Introduction

Cognitive decline in type 2 diabetes mellitus (T2DM) has been shown in both human patients and experimental animal models.[1] Multiple mechanisms such as metabolic dysfunction, vascular abnormalities, neuroinflammation, and synaptic degeneration have been shown to influence the cognitive decline in genetic- or diet-induced obesity.[2–4] However, finding effective therapeutic targets is difficult due to the complexity of disease pathology.

[1]Department of Anatomy and Convergence Medical Science, Institute of Health Sciences, Gyeongsang National University School of Medicine, Jinju, Republic of Korea
[2]Department of Neurology, Institute of Health Sciences, Gyeongsang National University School of Medicine, Gyeongsang National University Hospital, Jinju, Republic of Korea
[3]Department of Neurologic Surgery, Mayo Clinic College of Medicine, Rochester, USA
[4]Department of Medical Genetics, Ajou University School of Medicine, Suwon, Republic of Korea
[5]C&K genomics, Seoul, Republic of Korea
[6]Division of Metabolic Diseases, Center for Biomedical Sciences, National Institute of Health, Osong, Republic of Korea

*These authors contributed equally to this work.

Corresponding author:
Gu Seob Roh, Department of Anatomy and Convergence Medical Science, Gyeongsang National University School of Medicine, 15, Jinju-daero, 816 Beon-gil, Jinju, Gyeongnam 660-751, Republic of Korea.
Email: anaroh@gnu.ac.kr

Diabetes induces blood–brain barrier (BBB) leakage and neuroinflammation, which causes brain ischemic changes and atrophy.[5] Cognitive function was impaired in rats of a high-energy diet and disruption of BBB integrity was observed in the hippocampus.[6] Diabetes has also changed directly the hippocampal synaptic function. A genetically obese db/db mice exhibited reduced levels of microtubule-associated protein 2 and dendritic spine density.[7] Overactivity of glycogen synthase kinase-3β (GSK-3β) caused by impaired insulin signaling in diabetes produces hyperphosphorylation of tau and alters neuronal structure and synaptic function.[8,9] Inhibition of GSK3β activity restores hippocampal long-term potentiation (LTP) that is impaired in db/db mice.[10] Altered insulin and insulin-like growth factor expression in Alzheimer's disease (AD) brains is associated with reduction in choline acetyltransferase expression.[11] BBB leakage and vascular abnormalities may precipitate synaptic dysfunction in early stages of neurodegeneration and cognitive decline becomes manifest in T2DM patients.[12,13]

Calcium homeostasis is altered in diabetes and a causal relationship of hyperglycemia and calcium dysregulation has been reported in key insulin-responsive organs (skeletal muscle and liver) as well as heart and brain; the pathways are dependent on the activation of Ca^{2+}/calmodulin (CaM)-dependent protein kinase II (CaMKII) which was induced by mitochondrial reactive oxygen species, Ca^{2+} release from ER, and/or hyperglycemia-induced O-linked glycosylation.[14–16] Calpains, cysteine proteases, are also involved in metabolic dysfunction associated with diabetes[17] where hyperglycemia induces intracellular Ca^{2+} overload and calpain activation. However, the molecular mechanisms of hippocampal Ca^{2+} dysregulation and cognitive deficits associated with hyperglycemia have not been determined.[18] Due to the role of Ca^{2+}/CaM signaling in synaptic plasticity, a variety of factors in dentritic spines of hippocampal neurons are considered to regulate cognitive function. Neurogranin (Ng) is abundantly expressed in cortical and hippocampal neurons and particularly localized at dendritic spines.[19] Ng is a CaM-binding protein and recruits Ca^{2+}/CaM signaling to postsynaptic regions, where Ng potentiates N-methyl-D-aspartate receptor (NMDAR)-mediated synaptic transmission.[20] Ng knockout mice exhibit a severe deficit in LTP induction and poor performance in spatial learning tasks, whereas Ng overexpression in CA1 neurons enhances synaptic strength and LTP induction.[20,21]

Caloric restriction (CR) is the most robust nongenetic metabolic intervention that treats age-related diseases and increases lifespan in different model organisms.[22] The beneficial effects of CR or CR mimetics are through reducing metabolic and oxidative stress, inflammation, and neurodegeneration.[23,24] CR increases hippocampal dendritic spine density and neutrophin levels in db/db mice.[25] CR prevents aging-associated Ca^{2+} dysregulation in CA1 pyramidal neurons and may protect against synaptic dysfunction in aged animals,[26] which may explain the beneficial effect of CR on diabetes-induced memory deficits.

In this study, we investigated molecular mechanisms of CR-mediated neuroprotection by regulating Ca^{2+} signaling. We showed in the RNA-seq analysis that Ng was down-regulated in the hippocampus of HFD-fed mice and we explored whether Ng signaling is involved in diabetes-induced cognitive dysfunction and benefits of CR. Here we report that CR improved diabetes-induced cognitive deficits by regulating Ng-associated Ca^{2+} signaling.

Materials and methods

Human subjects

The case–control study was conducted at Gyeongsang National University Hospital (GNUH) from January 2011 to July 2013 and approved by the local IRB (IRB No. 2013-12-014). Written consent was obtained from all participants. A total of 55 patients with T2DM (average disease duration 7.91 ± 6.35 years) and 64 normal subjects with normal cognitive status were enrolled in the study (Supplementary Table 1). None of the subjects had abnormal neurologic signs or symptoms or a history of neurologic or psychiatric illness. Patients with T2DM receiving antidiabetic treatments were included, but patients who were receiving insulin treatment or had uncontrolled hyperglycemia, complicated diabetes, or history of severe and frequent hypoglycemic events were excluded.

Assessment of cognitive functions and brain structural changes

Cognitive function was assessed using Korean version Mini-Mental State Examination (K-MMSE), clinical dementia rating, and Geriatric Depression Scale (GDS). All tests were performed by one trained clinical neuropsychologist at GNUH. Sixty-four percent (n = 35) of T2DM patients and 58% (n = 37) of normal subjects underwent brain MRI scans (1.5 Tesla, Siemens, Erlangen, Germany). Axial T2 and T1, fluid-attenuated inversion recovery (FLAIR) images (5 mm thick), and coronal T1-weighted images (1.5 mm thick) were obtained. The ischemic changes were rated separately by two neurologists using the Scheltens scale on axial T2 or FLAIR images.[27] The atrophy of medial temporal lobe in T1-weighted coronal images was rated using the Scheltens scale.[28]

HFD-induced obesity and CR animal model

Male C57BL/6 mice (three weeks old) were purchased from KOATECH (Pyeongtaek, South Korea) and maintained in the animal facility at Gyeongsang National University (GNU). Animal experiments were performed in accordance with the National Institutes of Health Guidelines on the Use of Laboratory Animals. The Animal Care Committee for Animal Research of GNU approved the study protocol (GNU-130306-M0021). Mice were housed in a 12 h light/12 h dark cycle. For HFD-induced obesity model, mice were divided into two groups (n = 15 per group) at four weeks of age and fed either a high-fat diet (HFD, 60 kcal% fat, 5.24 kcal/g, Research Diets, Inc., New Brunswick, NJ) or normal standard diet chow (ND, 2018S, 3.1 kcal/g, Harlan Laboratories, Inc., Indianapolis, IN) for 40 weeks. For CR model, mice were divided into three groups (n = 15 per group) at four weeks of age and fed either a HFD or ND for 20 weeks. Mice were transferred to individual cages and continued on the HFD or subjected to caloric restriction (CR, 2 g/day of HFD) for 12 weeks. The total caloric intake of CR diet was comparable to that of ND (p = 0.23) and the total caloric intake of HFD+CR was restricted to ~70% of the HFD.[29,30] Mice were weighed monthly and before sacrifice.

Glucose tolerance test (GTT) and insulin tolerance test (ITT)

GTT and ITT were performed as previously described.[15] Briefly, D-glucose (2 g/kg, Sigma-Aldrich, St. Louis, MO, USA) or insulin (0.75 U/kg, Humulin-R, Eli Lilly, Indianapolis, IN, USA) was injected and blood glucose was measured before and after the injection using an Accu-Chek glucometer (Roche Diagnostics GmbH, Mannheim, Germany).

Measurement of serum metabolic parameters

Mice were anesthetized with zoletil (5 mg/kg, Virbac Laboratories, Carros, France) and blood samples (n ≥ 8 per group) were collected transcardially. Serum glucose, aspartate aminotransferase, alanine aminotransferase, free fatty acids, and total cholesterol levels were determined in Green Cross Reference Laboratory (Yongin-si, South Korea). Serum insulin, leptin, and adiponectin (n = ≥ 8 per group) were measured using mouse insulin (Shibayagi Co., Gunma, Japan), leptin (Crystal Chem Inc., IL, USA), and adiponectin (Shibayagi) enzyme-linked immunosorbent assay kits.

Tissue collection and sample preparation

For tissue analysis, mice (n = 6 per group) were anesthetized with zoletil (5 mg/kg, Virbac Laboratories) and perfused by 4% paraformaldehyde in 0.1 M PBS. After 6 h of fixation, the brains were sequentially immersed in 15 and 30% sucrose at 4°C until they sank. The brains were sliced into 40 μm coronal sections. Liver and epididymal fat pads were processed for paraffin embedding, sliced into 5 μm sections, and stained with H&E (Sigma-Aldrich). The sections were visualized under a BX51 light microscope (Olympus, Tokyo, Japan).

Fluoro-Jade B Staining

To evaluate neurodegeneration, Fluoro-Jade B (FJB; Chemicon International, CA, USA) staining was performed according to the manufacturer's instructions. FJB-positive degenerating neurons were visualized under a confocal microscope (FV-1000, Olympus) as green fluorescent cells.

Double immunofluorescence

The frozen free-floating brain sections were incubated with primary antibodies (Supplementary Table 2), and after washing, the sections were incubated with Alexa Fluor 488- and 594-conjugated donkey anti-rabbit or anti-mouse secondary antibodies (Invitrogen, CA, USA). Fluorescence was visualized under a confocal microscope (FV-1000, Olympus).

Immunohistochemistry

After serum blocking, frozen brain sections were incubated with primary antibodies (Supplementary Table 2) and then with secondary biotinylated antibodies. After washing, sections were incubated in avidin–biotin–peroxidase complex solution (Vector Laboratories, Burlingame, CA, USA) and developed with diaminobenzidine (Sigma-Aldrich). The sections were dehydrated through graded alcohols, cleared in xylene, and mounted.

Western blot analysis

Proteins were extracted from hippocampal tissues as described.[31] Proteins were separated via electrophoresis and transferred onto membranes. Proteins were immunoblotted with primary antibodies (Supplementary Table 2) and visualized using ECL substrates (Pierce, Rockford, IL, USA). The Multi Gauge V 3.0 image analysis program (Fujifilm, Tokyo, Japan) was used for band densitometry.

Morris water maze test

Morris water maze test was performed as previously described.[31] Briefly, mice ($n \geq 10$ per group) were trained to find a hidden platform as four trials per day for four consecutive days. The escape latency was recorded by a video-tracking program (Noldus EthoVision XT7, Noldus Information Technology, Netherlands).

Next generation sequencing (NGS)-based RNA-seq analysis

C&K genomics (Seoul, South Korea) performed preparation of RNA-seq library, sequencing, and bioinformatics analysis. Briefly, sequencing was performed by Illumina HiSeq2000 and the quality-filtered reads were aligned to Mus_musculus genome (GRCm38) from Ensembl database. The R package DESeq[32] was used to find differentially expressed genes (DEGs) ($p < 0.01$) which were then converted to official gene symbols and grouped by a common biological property according to Gene Ontology (GO) and Kyoto Encyclopedia of Genes and Genomes (KEGG) pathway analyses. The enriched GO terms were used to functionally cluster DEGs which were then filtered ($p < 0.05$). The RNA sequencing data from this study have been deposited under the NCBI Project Accession Number: PRJNA261860.

Quantitative real-time reverse-transcription PCR

Total RNAs were isolated using TRIzol reagent (Invitrogen, Carlsbad, CA, USA) and reverse-transcribed using the RevertAid[TM] First-Strand cDNA Synthesis Kit (Fermentas Inc., Hanover, MD, USA). Real-time RT-PCR was performed using the ABI Prism 7000 Sequence Detection System (Applied Biosystems, Foster City, CA, USA). PCR amplifications were performed using the SYBR Green I qPCR kit (TaKaRa, Shiga, Japan) with specific primers: 5′-TCCAAGCC AGACGACGATATT-3′ and 5′-CACACTCTCCGCT CTTTATCTTC-3′ for mouse *Ng* (GenBank: NM_ 022029), and 5′-TGACCACAGTCCATGCCATC-3′ and 5′-GACGGACACATTGGGGGTAG-3′ for mouse *Gapdh* (GenBank: NM_001289726).

Statistics

For the human study, IBM SPSS statistics 21 was used. The T2DM was treated as a dichotomized variable. Continuous variables were analyzed using independent t-test or Welch–Aspin test, and categorical variables were analyzed using Pearson χ^2-test. For the mouse study, Student's t-test or two-way ANOVA followed by Bonferroni post hoc analysis was used.

Results

Cognitive function and brain structure of T2DM patients

We accessed clinical characteristics and cognitive functions in 55 patients diagnosed with T2DM and 64 normal subjects (Supplementary Table 1 and Table 1). Overall scores obtained by K-MMSE and GDS were not different between T2DM and normal subjects (Table 1). However, T2DM patients had significant deficits in visuospatial function assessed by Rey Complex Figure Test copy, memory function assessed by Seoul Verbal Learning Test-delayed recall (SVLT-DR), and frontal/executive function assessed by contrast program (P2 < 0.05; P2, p-value adjusted for age, gender, education, and hypertension).

To relate the cognitive functional deficits to structural changes in the brains of T2DM patients, MRI was performed. Representative Scheltens ischemic scales on T2-weighted and FLAIR axial images are displayed in Supplementary Figure 1. T2DM patients displayed severe ischemic changes in lobar white matter hyperintensities and infratentorial foci relative to normal subjects (P2 < 0.05) (Table 2). Total Scheltens ischemic scores were also higher in T2DM patients than in normal subjects (P2 < 0.05) and there was a significant correlation between the SVLT-DR and ischemic changes ($r = -0.4$, $p < 0.05$).

Memory deficits and BBB leakage in HFD-fed mice

To investigate molecular mechanisms of the diabetes-induced cognitive decline observed in human study, mice were fed a HFD for 40 weeks to induce obesity-induced diabetes (Supplementary Figure 2). The body weight and fasting blood glucose levels were higher in HFD-fed mice than in ND-fed mice (Supplementary Figure 2(a) and (b)), and the insulin and glucose tolerances were impaired in HFD-fed mice (Supplementary Figure 2(c) and (d)). HFD-fed mice exhibited hypoadiponectinemia, hyperinsulinemia, and hyperleptinemia (Supplementary Figure 2(e) to (g)). The chronic HFD feeding significantly increased expression of proteins involved in inflammation, glial activation, and BBB leakage, which was confirmed by western blotting of inflammation markers, high-mobility group protein B1, receptor for advanced glycation endproducts, toll-like receptor 4, and COX-2 (Supplementary Figure 3(a) and (b)). The glial activation and BBB leakage were confirmed by western blotting of Iba-1, glial fibrillary acidic protein, IgG, and vascular endothelial growth factor (VEGF) (Supplementary Figure 3(c) and (d)). The phenotype of HFD-fed mice agreed with the brain ischemic changes present in T2DM patients.

Table 1. Assessment of neuropsychological functions in T2DM and normal subjects.

	Type 2 diabetes (N = 55)	Normal (N = 64)	P1	P2
K-MMSE	25.05 ± 0.48	25.81 ± 0.42	0.235	0.745
GDS	16.72 ± 1.14	15.42 ± 1.05	0.4	0.674
Attention				
Digit span_Forward	5.96 ± 0.24	6.43 ± 0.18	0.11	0.256
Digit span_Backward	3.35 ± 0.20	3.84 ± 0.17	0.057	0.076
Language related function				
K_BNT	43.85 ± 1.22	46.19 ± 1.11	0.161	0.391
Calculation	9.89 ± 0.37	10.73 ± 0.20	*0.039*	0.109
Ideomotor apraxia	4.91 ± 0.05	4.84 ± 0.07	0.461	0.554
Visuospatial function				
RCFT_copy	25.84 ± 0.87	28.28 ± 0.58	*0.019*	*0.047*
Memory function				
SVLT_IR	18.28 ± 0.72	20.27 ± 0.70	0.051	0.373
SVLT_DR	4.89 ± 0.40	6.5 ± 0.32	*0.002*	*0.018*
SVLT_REG	19.29 ± 0.35	20.58 ± 0.31	*0.007*	0.059
RCFT_IR	10.88 ± 0.88	12.43 ± 0.79	0.177	0.348
RCFT_DR	10.07 ± 0.82	12.4 ± 0.79	*0.044*	0.089
RCFT_REG	18.07 ± 0.35	18.97 ± 0.27	*0.044*	0.071
Frontal/executive function				
Contrast program	19.27 ± 0.27	19.92 ± 0.03	*0.019*	*0.018*
Go_No_Go test	18.2 ± 0.43	19.16 ± 0.30	0.068	0.1
COWAT_Animal	13.6 ± 0.49	14.16 ± 0.48	0.42	0.75
COWAT_Supermarket	11.13 ± 0.57	12.64 ± 0.58	0.068	0.315
COWAT_Phonemic	17.42 ± 1.40	20.52 ± 1.43	0.127	0.176
Strooptest_Color reading	69.2 ± 3.69	81.05 ± 2.91	*0.012*	0.112

COWAT: Controlled Oral Word Association Test; GDS: Geriatric Depression Scale; IR/DR/REG: immediate recall/delayed recall/recognition; K-BNT: Korean version Boston Naming Test; K-MMSE: Korean version Mini-Mental State Examination; RCFT: Rey Complex Figure Test; SVLT: Seoul Verbal Learning Test. Data are presented as mean ± SEM. $P < 0.05$ (shown in italics) for T2D versus normal subjects. P1 was calculated by independent t-test and P2 was calculated by ANCOVA adjusted by age, gender, education, and hypertension.

Table 2. Assessment of Scheltens ischemic rating scales in T2DM and normal subjects.

	Type 2 Diabetes (N = 35)	Normal (N = 37)	P1	P2
PVH	2.63 ± 0.35	1.79 ± 0.32	0.082	0.236
WMH	4.49 ± 0.83	2.09 ± 0.36	*0.011*	*0.023*
BG	1.34 ± 0.34	0.54 ± 0.16	*0.038*	0.056
ITF	0.34 ± 0.11	0.06 ± 0.04	*0.017*	*0.032*
Total ischemic scores	8.8 ± 1.38	4.31 ± 0.68	*0.005*	*0.013*

BG: basal ganglia; ITF: infratentorial foci; PVH: periventricular hyperintensities; WMH: lobar white matter hyperintensities. Data are presented as mean ± SEM. $P < 0.05$ (shown in italics) for T2D versus normal subjects. P1 values were calculated by independent t-test. P2 values were calculated by ANCOVA adjusted by age, gender, education, and hypertension.

Differential gene expression in the hippocampus of HFD-fed mice

To identify molecules responsible for diabetes-induced cognitive deficits, we conducted NGS-based RNA-seq analysis and examined hippocampal gene expression profiles in ND- and HFD-fed mice. We identified 90 DEGs (p < 0.01) and clustered them functionally by GO and KEGG pathway analyses (Figure 1(a) and (b)). The down- and up-regulated genes by HFD
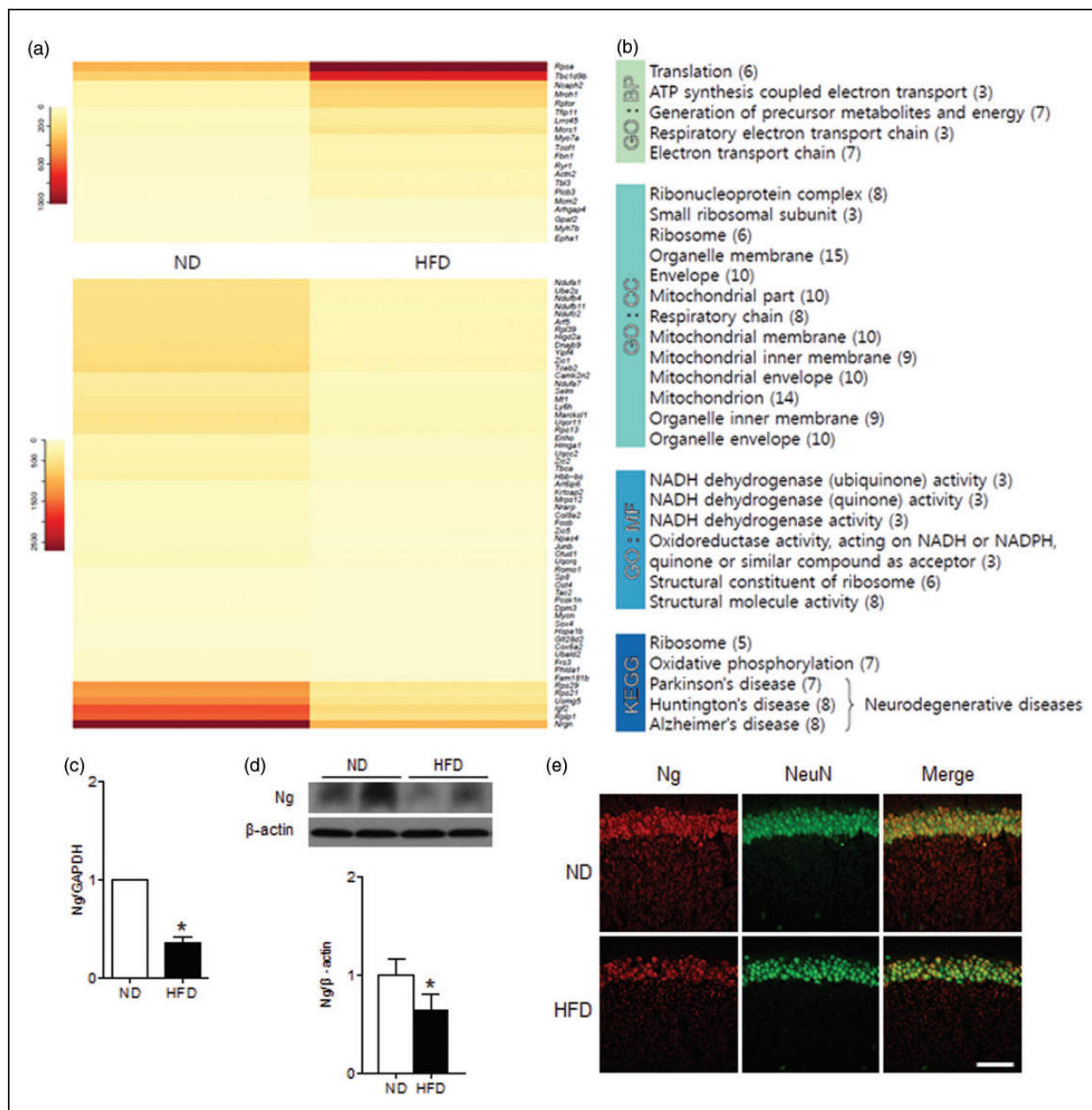
Figure 1. RNA-seq analysis of DEGs in the hippocampus of ND-fed and HFD-fed mice. (a) The differential expression of genes in ND-fed versus HFD-fed mice was color shaded after NGS-based RNA-seq analysis. Genes shown in red had up-regulated expression, and those shown in yellow had down-regulated expression (Supplementary Table 3). (b) The identified genes were functionally clustered by gene ontology (GO) analysis (biological process (BP), cellular component (CC), and molecular function (MF)) and Kyoto Encyclopedia of Genes and Genomes (KEGG) pathway analysis. (c) Relative gene expression of *Ng* is shown by qRT-PCR. (d) Protein expression of Ng is shown by western blots. Values were normalized by GAPDH or β-actin. (e) Immunofluorescence staining of Ng and NeuN. Data are presented as mean $\pm$ SEM. *p < 0.05 for HFD-fed versus ND-fed mice. Scale bar $= 100\,\mu m$.

feeding are listed in Supplementary Table 3. We found two down-regulated genes in Ca^{2+}/CaM-dependent signaling; Ng and CaMKII inhibitor 2 (Camk2n2). Ng is a CaM-binding protein that recruits Ca^{2+}/CaM signaling at dendritic spines and the reduced Ng expression in HFD-fed mice may alter intracellular Ca^{2+}/CaM

dynamics.[33] The reduced expression of Camk2n2, an endogenous CaMKII inhibitor,[34] may induce aberrant activation of CaMKII. We further examined Ng expression in mRNA and protein levels that were decreased in the hippocampus of HFD-fed mice (Figure 1(c) and (d)). The immunofluorescence staining
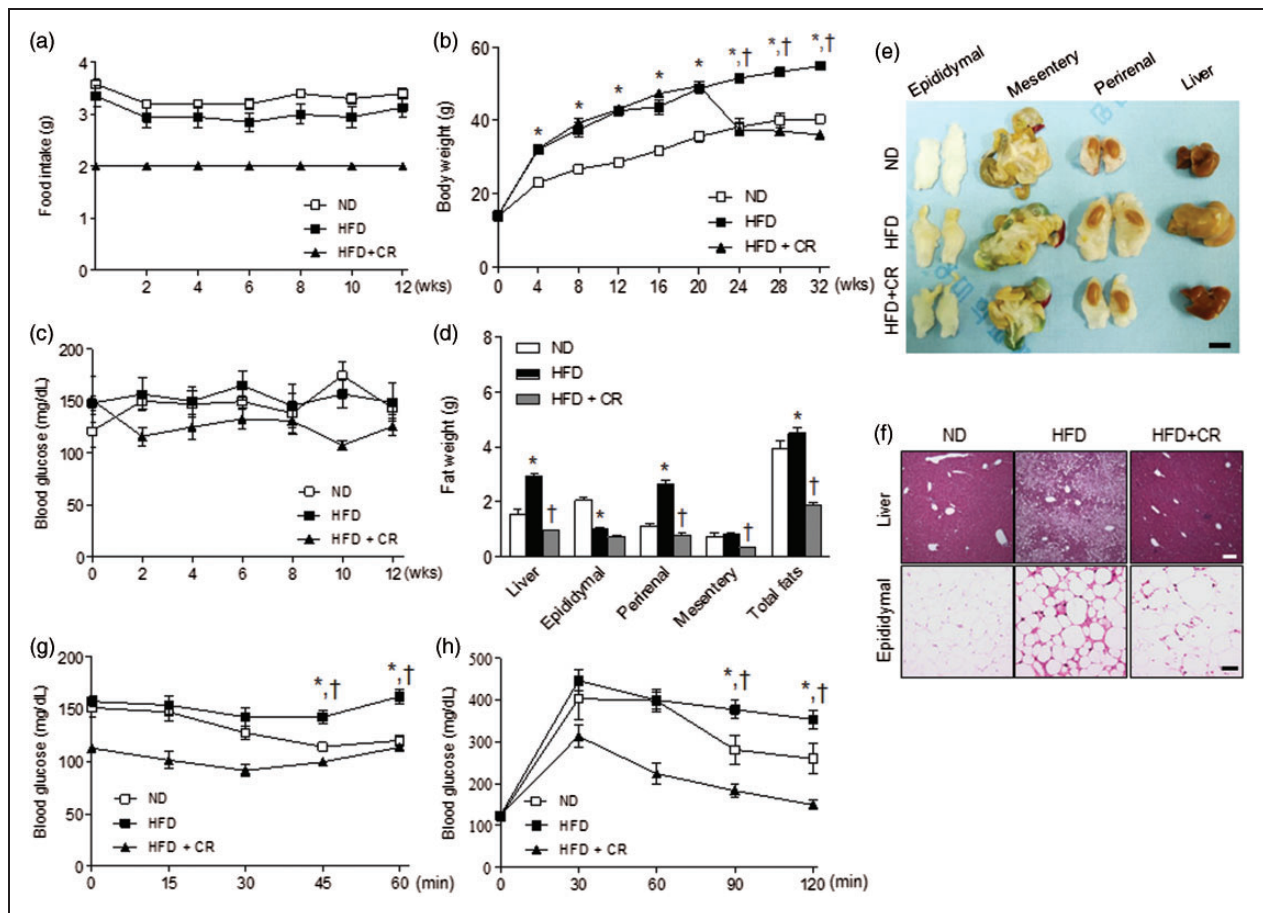
Figure 2. Effects of CR on the diabetic phenotype of HFD-fed mice. (a) Food intake; (b) body weight; (c) fasting blood glucose; (d) weight changes in liver and intraabdominal fats (epididymal, mesentery, and perirenal fat); (e) gross morphology of liver and intraabdominal fats; (f) lipid accumulation in hepatocytes and macrophage infiltration in adipocytes shown by H&E staining; and insulin (g) and glucose (h) tolerance tests in ND, HFD, and HFD-fed caloric-restricted (HFD+CR) mice. Data are presented as mean ± SEM. *$p < 0.05$ for HFD-fed versus ND-fed mice. †$p < 0.05$ for HFD+CR versus HFD-fed mice. Scale bar = 1 cm (in (e)), or 100 μm (in (f)).

of Ng showed a decrease of neuron-specific Ng expression in the CA1 region of HFD-fed mice (Figure 1(e)).

Effects of CR on metabolic phenotype in HFD-fed mice

CR decreases obesity-induced metabolic stress and the CR effect on diabetes-induced cognitive deficits was investigated. We first examined the metabolic phenotype of HFD-fed mice with and without CR (2 g/day) (Figure 2(a)). The total caloric intake of 2 g of HFD+CR mice is comparable to that of ND group ($p = 0.23$). The total calorie intake of HFD-fed mice was $52.8 \pm 1.6\%$ ($P < 0.05$) higher than ND-fed mice and the total calorie intake of HFD+CR mice was restricted to $67.2 \pm 4.5\%$ ($P < 0.05$) of the HFD mice (Supplementary Figure 4). Body weight was significantly lower in HFD+CR mice than in HFD-fed mice and was similar to the level of ND-fed mice (Figure 2(b)). However, nonfasting blood glucose was

not significantly different among the groups (Figure 2(c)). The weights of liver and perirenal fat were significantly lower in HFD+CR mice than in HFD-fed mice (Figure 2(d)), and the sizes of liver and perirenal fat in HFD+CR were similar to them in ND-fed mice (Figure 2(e)). The lipid accumulation in hepatocytes and the macrophage infiltration in adipocytes of HFD-fed mice were significantly reduced by CR (Figure 2(f)). ITT and GTT demonstrated that HFD+CR mice improved in blood glucose regulation compared with HFD-fed mice (Figure 2(g) and (h)). In addition, CR significantly reversed serum metabolic parameters in HFD-fed mice (Table 3).

Effects of CR on glial activation, BBB leakage, and memory deficits in HFD-fed mice

We examined whether CR has a protective effect on HFD-induced glial activation and BBB leakage by western blot analysis (Figure 3(a) and (b)). CR reduced

Table 3. Serum metabolic parameters in ND-fed and HFD-fed mice with and without CR.

	ND (n = 8)	HFD (n = 13)	HFD + CR (n = 15)
Leptin (ng/ml)	23.63 ± 1.97	44.44 ± 1.43[*]	13.60 ± 1.19[†]
Insulin (ng/ml)	0.47 ± 0.17	1.22 ± 0.18[*]	0.32 ± 0.03[†]
Glucose (mg/dl)	406.50 ± 49.82	505.77 ± 33.37[*]	316.80 ± 24.00[†]
HOMA-IR	7.40 ± 0.53	36.68 ± 5.08[*]	6.22 ± 0.77[†]
Adiponectin (µg/ml)	56.85 ± 13.72	31.11 ± 6.19[*]	79.65 ± 10.94[†]
AST (U/l)	106.25 ± 13.78	220.23 ± 10.98[*]	124.13 ± 11.86[†]
ALT (U/l)	43.00 ± 10.52	255.31 ± 24.02[*]	23.60 ± 1.23[†]
Total cholesterol (mg/dl)	131.25 ± 7.76	283.46 ± 10.41[*]	141.53 ± 7.97[†]
Free fatty acid (µEq/l)	1192.75 ± 51.36	1268.31 ± 47.72[*]	1004.47 ± 58.61[†]

The homeostasis model assessment of insulin resistance (HOMA-IR) was calculated from the fasting blood glucose (mmol/l) × fasting plasma insulin (µU/ml) divided by 22.5. Data are presented as the mean ± SEM. [*]$P < 0.05$ for HFD-fed versus ND-fed mice, [†]$P < 0.05$ for HFD+CR versus HFD-fed mice.

the HFD-induced expression of Iba-1 (Figure 3(a)). We found a slight increase in the size of Iba-1-expressing cells in the hippocampus of HFD-fed mice; however, there was no dramatic morphological changes shown in activated phagocytic microglia–maximally immune responsive microglia (Supplementary Figure 5(a)). The number of microglial cells was significantly increased (∼10%, p < 0.05) in HFD-fed mice and reduced by CR treatment (Supplementary Figure 5(b)). CR also reduced HFD-induced expression of IgG and VEGF indicating that CR may reduce glial activation and BBB leakage (Figure 3(b)). We also examined GSK-3β which is highly activated in many neurodegenerative diseases.[9] The level of phosphorylated GSK-3β, the inactive form was decreased in HFD-fed mice and was reversed by CR (Figure 3(c)).

We further examined the CR effect on memory deficits in HFD-fed mice. In the Morris water maze test, HFD+CR mice exhibited reduced escape latencies during training trials and increased the time spent in the target quadrant during probe tests, compared with HFD-fed mice (Figure 3(d) and (e)). The swimming trajectories demonstrated more directed movements to the target quadrant in HFD+CR mice than in HFD-fed mice where the trajectories were spread out over all quadrants (Figure 3(f)). The swim speed analysis showed no significant difference among the groups during four days of training trials and probe tests (Supplementary Figure 6(a)). This indicates that the results are not due to the delayed movements of HFD-fed mice. We also analyzed the distance moved during training days in Supplementary Figure 6(b). The distance moved by HFD-fed mice was not significantly reduced along the training days (p = 0.23), indicating that HFD-fed mice were delayed in learning. ND-fed and HFD+CR mice showed a significant decrease in the distance moved along the training days (p < 0.05).

The results suggest that CR improved the spatial learning and memory deficits induced by HFD.

Effects of CR on the expression of Ng and downstream proteins in HFD-fed mice

To investigate the molecular mechanism of CR on diabetes-induced cognitive deficits that are mediated by Ng signaling, we examined the expression of Ng and downstream proteins. CR reversed the HFD-induced decrease in Ng to the levels of ND-fed mice (Figure 4(a)). Ng-positive cells were examined in the CA1 hippocampal neurons (Figure 4(b)). Ng immunoreactivity was significantly reduced (∼30%, p < 0.05) in HFD-fed mice and recovered by CR (ND 100 ± 5.07%, HFD 70.5 ± 8.35%, and HFD+CR 99.2 ± 5.56%). We additionally performed FJB staining to detect neurodegenerating neurons present in HFD mice compared with ND or HFD+CR mice; however, there was no sign of neurodegeneration in the hippocampus of HFD mice (data not shown). The gross morphology of hippocampus and NeuN staining was not altered by HFD. The results indicate that reduced Ng expression is not due to neuronal loss.

The phosphorylated CaMKII (p-CaMKII) that are activated by Ca^{2+} was abnormally increased in HFD-fed mice and decreased by CR (Figure 4(c)). The reduced expression of Camk2n2 may also contribute to the abnormal CaMKII activity in hippocampus of HFD-fed mice. The activity of calpain, a Ca^{2+}-dependent cysteine protease, was accessed by the cleavage of p35 to p25 (Figure 4(d)) and the fragmentation of α-spectrin (Figure 4(e)). The activity of cAMP responsive-element binding (CREB)-1, a downstream effector of p-CaMKII was also accessed by the phosphorylation levels (Figure 4(f)). The p25, α-spectrin fragment, and phosphorylated CREB-1 levels were all increased in
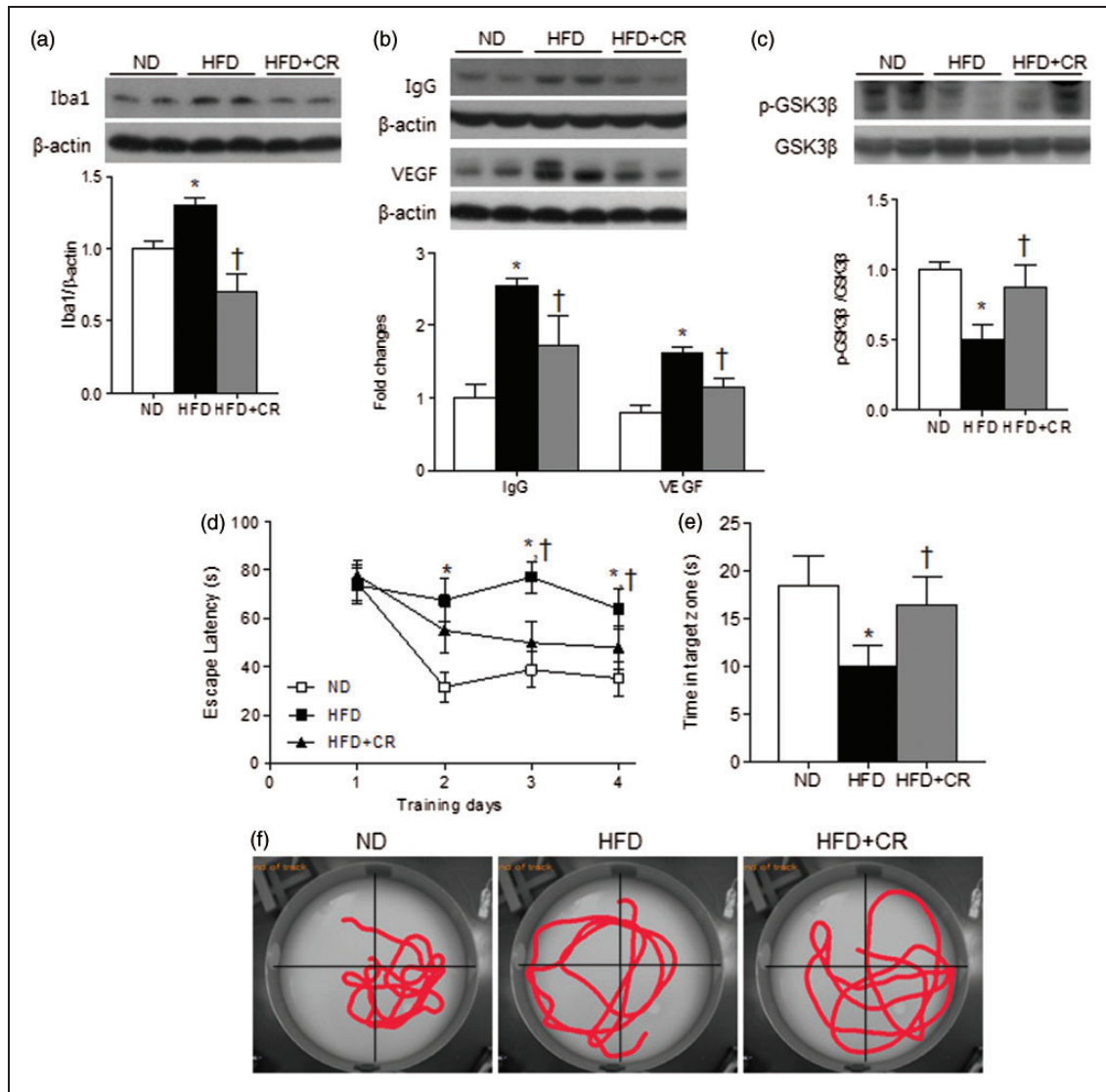
Figure 3. Effects of CR on glial activation, BBB leakage, and memory deficits in HFD-fed mice. Representative western blots and protein quantification of (a) Iba-1, (b) IgG and VEGF, and (c) p-GSK3β in the hippocampus of ND, HFD, and HFD+CR mice. Band intensity was normalized to β-actin or GSK3β. (d) Escape latency over four days of training trials; (e) average time spent in the target zone during probe trials; and (f) representative swimming trajectories of ND, HFD, and HFD+CR mice. Data are presented as mean ± SEM. *$p < 0.05$ for HFD-fed versus ND-fed mice. †$p < 0.05$ for HFD+CR versus HFD-fed mice.

HFD-fed mice, which were reversed by CR. The results suggest that CR attenuated the HFD-induced up-regulation of Ca^{2+}-dependent signaling and stimulation of CaMKII and calpain activity.

Discussion

This study demonstrated the mild cognitive impairment (MCI) and correlative ischemic changes in T2DM patients and consistently in HFD-fed mice that showed significant memory deficits and molecular changes associated with glial activation and BBB leakage. To search molecular targets associated with

diabetes-induced cognitive deficits, we performed RNA-seq analysis in the hippocampus of HFD-fed mice. Ng was down-regulated by HFD feeding and further investigated due to its synaptic function. CR treatment improved HFD-induced memory deficits and BBB leakage and normalized Ng expression and associated calcium signaling. These findings suggest that CR improves diabetes-induced cognitive deficits by attenuating Ng-associated calcium signaling.

In this study, T2DM patients showed significant cognitive decline, in particular, the memory, visuospatial, and frontal/executive dysfunction. There was ischemic brain change, but no atrophy in the medial
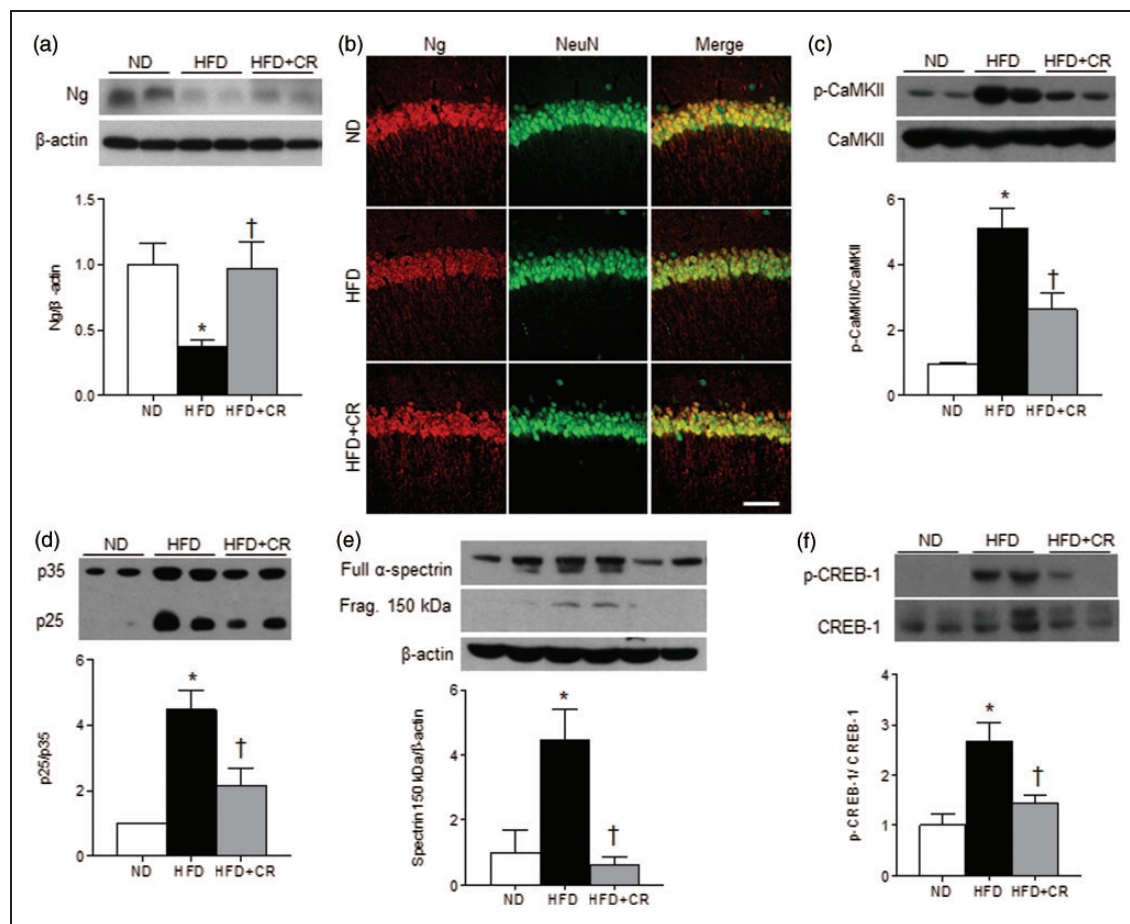
Figure 4. Effects of CR on the hippocampal expression of Ng and downstream proteins. Representative western blots and protein quantification of (a) Ng in the hippocampus of ND, HFD, and HFD+CR mice. (b) Immunofluorescence staining of Ng in the hippocampal CA1 region. Representative western blots and protein quantification of (c) p-CaMKII and CaMKII, (d) p35 and p25, (e) full length α-spectrin and the fragment, and (f) p-CREB-1 and CREB-1. Data are presented as mean ± SEM. *p < 0.05 for HFD-fed versus ND-fed mice. †p < 0.05 for HFD+CR versus HFD-fed mice. Scale bar = 100 μm.

temporal lobe of the T2DM patients, suggesting that these individuals have MCI rather than dementia. The ischemic changes are derived from vascular abnormalities often caused by abnormal structure and function of BBB, the permeability of which is significantly altered in diabetes, which causes insufficient transport of metabolites and signaling molecules and neuronal energy failure.[5] Consistently, HFD-fed mice showed significant memory deficits and increased BBB leakage and glial activation; the defects were normalized by CR treatment.

T2D often coexists with other metabolic disturbances that increase risk of cognitive impairment, such as hypertension and dyslipidemia. Several studies have shown that hypertensive patients with T2D have pronounced cognitive dysfunction on neurological tests compared to normotensive diabetic patients.[35] Cognitive performance is also correlated with glucose tolerance status in the elderly, suggesting that improving

glucose control may reduce cognitive decline.[36] However, intensive blood pressure control, hypolipidemic agents, and glucose lowering medication do not always reduce cognitive decline because the synaptic and vascular changes are often irreversible.[37,38] The T2D patients in our study had relatively well-controlled glucose, lipids, and blood pressure, which minimized diabetes-related comorbidities. Overall scores of K-MMSE and GDS tests were not significantly different in T2D patients than in healthy controls, although the former exhibited deficits in memory function as measured by SVLT-DR (P2 < 0.05). However, multiple indicators of memory function were significantly low in T2D patients before adjusting for age, gender, education, and hypertension (P1 < 0.05). Further analysis of MRI and neuropsychological test results from large patient samples may elucidate function-specific ischemic changes and variable-dependent neurological phenotypes in T2D patients.

We performed RNA-seq analysis to identify DEGs associated with diabetes and cognitive dysfunction. The differential expression of Ng in the hippocampus of HFD-fed mice was noteworthy in that Ng regulates synaptic function and may explain HFD-induced memory deficits. There is a clear correlation with the Ng levels and cognitive function as previously shown in Ng knockout mice and overexpression studies.[20,21,39] Ng is decreased in the hippocampus of mouse models and patients with AD,[40,41] and was consistently down-regulated in the hippocampus of HFD-fed mice that performed poorly in Morris water maze test. The Ng level was restored to normal after CR treatment. Thus, diabetes-induced cognitive deficits may be closely associated with the reduced expression of Ng. CR may reduce metabolic stress and restore Ng expression to improve Ng-mediated synaptic function.

Ng is a protein kinase C substrate and the activity is regulated by phosphorylation[42]; however, there was no change in the level of phosphorylated Ng in our study (data not shown). However, we found a significant induction of CaMKII and calpain activity in the hippocampus of HFD-fed mice. CaMKII binds to and phosphorylates tau and amyloid precursor protein, being involved in the neurofibrillary degeneration of AD.[43] Aberrant CaMKII activation has previously shown in ATRX mutant mice that mimic a human mental retardation disorder; the pathology depends on the activation of Rac1-guanine nucleotide exchange factors, CaMKII substrates, which induces abnormal actin polymerization during dendritic spine formation.[44] The endogenous CaMKII inhibitors specifically block CaMKII activity and regulate CaMKII and NMDAR association during memory formation.[45] Calpain is abnormally activated in AD brain and calpain inhibitors have shown to improve memory and synaptic transmission.[46,47] We speculate that calpain activation in the hippocampus of HFD-fed mice also contributes synaptic dysfunction and memory deficits.

A chronic change in neuronal Ca^{2+} homeostasis in the hippocampus of HFD-fed mice is associated with hyperglycemia-induced metabolic dysfunction[48]; however, the direct targets are unknown. Our data showed a dramatic induction of phosphorylated CREB-1 levels in the HFD-fed mice, suggesting that the expression of CREB-1 target genes is affected. Neuropeptide Y and the receptors or neurotrophic factors have been reported as the CREB-1 targets and known to regulate food intake and energy homeostasis.[49,50] We suggest that the phosphorylated CaMKII aberrantly activates the transcriptional activity of CREB-1 and induces metabolic dysfunction in HFD-fed mice. We speculate that Ng interacts with CaMKII and modulates the activity of CREB-1 signaling pathway. Consistently, a previous study reported that a single-nucleotide polymorphism that was strongly associated with T2DM interacts with CaMKII and triggers CREB-1 phosphorylation and induction of the downstream target genes.[51]

The molecular mechanisms involved in CR-mediated cognitive improvement are largely unknown; however, CR-induced mild neuronal stress response may stabilize key molecules in synaptic plasticity and neurogenesis and protect from various stresses (e.g. oxidative stress, mitochondrial and ER stress, and toxic protein accumulation).[52] Thus, CR may attenuate age-dependent cognitive functional decline and neurodegeneration. Here, we suggest that CR improves HFD-induced memory deficits by up-regulating Ng expression and this action involves a reduction of CaMKII and calpain activity and the downstream signaling that may regulate neuronal metabolism, survival, and plasticity, on which the molecular details need to be further investigated. The CR-mediated Ng-Ca^{2+} pathways provide new targets for developing therapeutic strategies for metabolic diseases, neurodegeneration, and aging.

Declaration of conflicting interests

The author(s) declared no potential conflicts of interest with respect to the research, authorship, and/or publication of this article.

Authors' contributions

HK, HK, RWH, BTJ, CY, HJS conducted experiments and data analyses. JK, SYJ, WK performed RNA-seq analysis. WHK and SSK discussed the data. HK, HK, and GSR wrote the article and HK and HK equally contributed to the study.

Supplementary material

Supplementary material for this paper can be found at http://jcbfm.sagepub.com/content/by/supplemental-data

References

1. Strachan MW, Reynolds RM, Marioni RE, et al. Cognitive function, dementia and type 2 diabetes mellitus in the elderly. *Nat Rev Endocrinol* 2011; 7: 108–114.

2. Biessels GJ, Staekenborg S, Brunner E, et al. Risk of dementia in diabetes mellitus: a systematic review. *Lancet Neurol* 2006; 5: 64–74.

3. Kroner Z. The relationship between Alzheimer's disease and diabetes: type 3 diabetes? *Alternat Med Rev* 2009; 14: 373–379.

4. Nguyen JC, Killcross AS and Jenkins TA. Obesity and cognitive decline: role of inflammation and vascular changes. *Front Neurosci* 2014; 8: 375.

5. Huber JD. Diabetes, cognitive function, and the blood-brain barrier. *Curr Pharm Des* 2008; 14: 1594–1600.

6. Kanoski SE, Zhang Y, Zheng W, et al. The effects of a high-energy diet on hippocampal function and blood-brain barrier integrity in the rat. *J Alzheimer's Dis* 2010; 21: 207–219.

7. Chen J, Liang L, Zhan L, et al. ZiBuPiYin recipe protects db/db mice from diabetes-associated cognitive decline through improving multiple pathological changes. *PLoS One* 2014; 9: e91680.

8. Hooper C, Killick R and Lovestone S. The GSK3 hypothesis of Alzheimer's disease. *J Neurochem* 2008; 104: 1433–1439.

9. Zhou FQ and Snider WD. Cell biology. GSK-3beta and microtubule assembly in axons. *Science* 2005; 308: 211–214.

10. Huang S, Wang Y, Gan X, et al. Drp1-mediated mitochondrial abnormalities link to synaptic injury in diabetes model. *Diabetes* 2015; 64: 1728–1742.

11. Rivera EJ, Goldin A, Fulmer N, et al. Insulin and insulin-like growth factor expression and function deteriorate with progression of Alzheimer's disease: link to brain reductions in acetylcholine. *J Alzheimer's Dis* 2005; 8: 247–268.

12. Bowman GL, Kaye JA, Moore M, et al. Blood-brain barrier impairment in Alzheimer disease: stability and functional significance. *Neurology* 2007; 68: 1809–1814.

13. Kushner M, Nencini P, Reivich M, et al. Relation of hyperglycemia early in ischemic brain infarction to cerebral anatomy, metabolism, and clinical outcome. *Ann Neurol* 1990; 28: 129–135.

14. Erickson JR, Pereira L, Wang L, et al. Diabetic hyperglycaemia activates CaMKII and arrhythmias by O-linked glycosylation. *Nature* 2013; 502: 372–376.

15. Jain SS, Paglialunga S, Vigna C, et al. High-fat diet-induced mitochondrial biogenesis is regulated by mitochondrial-derived reactive oxygen species activation of CaMKII. *Diabetes* 2014; 63: 1907–1913.

16. Ozcan L, Cristina de Souza J, Harari AA, et al. Activation of calcium/calmodulin-dependent protein kinase II in obesity mediates suppression of hepatic insulin signaling. *Cell Metab* 2013; 18: 803–815.

17. Pandurangan M, Hwang I, Orhirbat C, et al. The calpain system and diabetes. *Pathophysiology* 2014; 21: 161–167.

18. Thibault O, Anderson KL, DeMoll C, et al. Hippocampal calcium dysregulation at the nexus of diabetes and brain aging. *Eur J Pharmacol* 2013; 719: 34–43.

19. Neuner-Jehle M, Denizot JP and Mallet J. Neurogranin is locally concentrated in rat cortical and hippocampal neurons. *Brain Res* 1996; 733: 149–154.

20. Zhong L, Cherry T, Bies CE, et al. Neurogranin enhances synaptic strength through its interaction with calmodulin. *EMBO J* 2009; 28: 3027–3039.

21. Huang KP, Huang FL, Jager T, et al. Neurogranin/RC3 enhances long-term potentiation and learning by promoting calcium-mediated signaling. *J Neurosci* 2004; 24: 10660–10669.

22. Arslan-Ergul A, Ozdemir AT and Adams MM. Aging, neurogenesis, and caloric restriction in different model organisms. *Aging Dis* 2013; 4: 221–232.

23. Chiba T, Tsuchiya T, Komatsu T, et al. Development of calorie restriction mimetics as therapeutics for obesity, diabetes, inflammatory and neurodegenerative diseases. *Curr Genom* 2010; 11: 562–567.

24. Merry BJ. Oxidative stress and mitochondrial function with aging—the effects of calorie restriction. *Aging Cell* 2004; 3: 7–12.

25. Stranahan AM, Lee K, Martin B, et al. Voluntary exercise and caloric restriction enhance hippocampal dendritic spine density and BDNF levels in diabetic mice. *Hippocampus* 2009; 19: 951–961.

26. Hemond P and Jaffe DB. Caloric restriction prevents aging-associated changes in spike-mediated Ca2+ accumulation and the slow afterhyperpolarization in hippocampal CA1 pyramidal neurons. *Neuroscience* 2005; 135: 413–420.

27. Scheltens P, Barkhof F, Leys D, et al. A semiquantitative rating scale for the assessment of signal hyperintensities on magnetic resonance imaging. *J Neurol Sci* 1993; 114: 7–12.

28. Scheltens P, Leys D, Barkhof F, et al. Atrophy of medial temporal lobes on MRI in "probable" Alzheimer's disease and normal ageing: diagnostic value and neuropsychological correlates. *J Neurol Neurosurg Psychiatry* 1992; 55: 967–972.

29. Hoevenaars FP, Keijer J, Herreman L, et al. Adipose tissue metabolism and inflammation are differently affected by weight loss in obese mice due to either a high-fat diet restriction or change to a low-fat diet. *Genes Nutr* 2014; 9: 391.

30. Ketonen J, Pilvi T and Mervaala E. Caloric restriction reverses high-fat diet-induced endothelial dysfunction and vascular superoxide production in C57Bl/6 mice. *Heart Vessels* 2010; 25: 254–262.

31. Jeon BT, Jeong EA, Shin HJ, et al. Resveratrol attenuates obesity-associated peripheral and central inflammation and improves memory deficit in mice fed a high-fat diet. *Diabetes* 2012; 61: 1444–1454.

32. Anders S and Huber W. Differential expression analysis for sequence count data. *Genome Biol* 2010; 11: R106.

33. Simons SB, Escobedo Y, Yasuda R, et al. Regional differences in hippocampal calcium handling provide a cellular mechanism for limiting plasticity. *Proc Natl Acad Sci USA* 2009; 106: 14080–14084.

34. Zhang J, Li N, Yu J, et al. Molecular cloning and characterization of a novel calcium/calmodulin-dependent protein kinase II inhibitor from human dendritic cells. *Biochem Biophys Res Commun* 2001; 285: 229–234.

35. Hassing LB, Hofer SM, Nilsson SE, et al. Comorbid type 2 diabetes mellitus and hypertension exacerbates

cognitive decline: evidence from a longitudinal study. *Age Ageing* 2004; 33: 355–361.

36. Yaffe K, Falvey C, Hamilton N, et al. Diabetes, glucose control, and 9-year cognitive decline among older adults without dementia. *Arch Neurol* 2012; 69: 1170–1175.

37. Launer LJ, Miller ME, Williamson JD, et al. Effects of intensive glucose lowering on brain structure and function in people with type 2 diabetes (ACCORD MIND): a randomised open-label substudy. *Lancet Neurol* 2011; 10: 969–977.

38. Williamson JD, Launer LJ, Bryan RN, et al. Cognitive function and brain structure in persons with type 2 diabetes mellitus after intensive lowering of blood pressure and lipid levels: a randomized clinical trial. *JAMA Intern Med* 2014; 174: 324–333.

39. Miyakawa T, Yared E, Pak JH, et al. Neurogranin null mutant mice display performance deficits on spatial learning tasks with anxiety related components. *Hippocampus* 2001; 11: 763–775.

40. George AJ, Gordon L, Beissbarth T, et al. A serial analysis of gene expression profile of the Alzheimer's disease Tg2576 mouse model. *Neurotox Res* 2010; 17: 360–379.

41. Reddy PH, Mani G, Park BS, et al. Differential loss of synaptic proteins in Alzheimer's disease: implications for synaptic dysfunction. *J Alzheimer's Dis* 2005; 7: 103–117. (discussion 173–180.

42. Kumar V, Chichili VP, Zhong L, et al. Structural basis for the interaction of unstructured neuron specific substrates neuromodulin and neurogranin with calmodulin. *Sci Rep* 2013; 3: 1392.

43. Wang JZ, Grundke-Iqbal I and Iqbal K. Kinases and phosphatases and tau sites involved in Alzheimer neurofibrillary degeneration. *Eur J Neurosci* 2007; 25: 59–68.

44. Shioda N, Beppu H, Fukuda T, et al. Aberrant calcium/calmodulin-dependent protein kinase II (CaMKII) activity is associated with abnormal dendritic spine morphology in the ATRX mutant mouse brain. *J Neurosci* 2011; 31: 346–358.

45. Lucchesi W, Mizuno K and Giese KP. Novel insights into CaMKII function and regulation during memory formation. *Brain Res Bull* 2011; 85: 2–8.

46. Saito K, Elce JS, Hamos JE, et al. Widespread activation of calcium-activated neutral proteinase (calpain) in the brain in Alzheimer disease: a potential molecular basis for neuronal degeneration. *Proc Natl Acad Sci USA* 1993; 90: 2628–2632.

47. Trinchese F, Fa M, Liu S, et al. Inhibition of calpains improves memory and synaptic transmission in a mouse model of Alzheimer disease. *J Clin Invest* 2008; 118: 2796–2807.

48. Biessels GJ, ter Laak MP, Hamers FP, et al. Neuronal Ca2+ disregulation in diabetes mellitus. *Eur J Pharmacol* 2002; 447: 201–209.

49. Fargali S, Sadahiro M, Jiang C, et al. Role of neurotrophins in the development and function of neural circuits that regulate energy homeostasis. *J Mol Neurosci* 2012; 48: 654–659.

50. Henry M, Ghibaudi L, Gao J, et al. Energy metabolic profile of mice after chronic activation of central NPY Y1, Y2, or Y5 receptors. *Obes Res* 2005; 13: 36–47.

51. Lin L, Hales CM, Garber K, et al. Fat mass and obesity-associated (FTO) protein interacts with CaMKII and modulates the activity of CREB signaling pathway. *Hum Mol Genet* 2014; 23: 3299–3306.

52. Fusco S and Pani G. Brain response to calorie restriction. *Cell Mol Life Sci* 2013; 70: 3157–3170.